ON THE TRANSMISSION OF BINARY BITS IN DISCRETE JOSEPHSON-JUNCTION ARRAYS

J. E. MACÍAS-DÍAZ AND A. PURI

ABSTRACT. In this work, we use supratransmission and infratransmission in the mathematical modeling of the propagation of digital signals in weakly damped, discrete Josephson-junction arrays, using energy-based detection criteria. Our results show an efficient and reliable transmission of binary information.

1. INTRODUCTION

The numerical study of wave transmission in long Josephson structures subject to harmonic driving was initiated in the middle 1980's by Olsen and Samuelsen [1], and the investigation was extended to coupled arrays of short superconducting tunnel junctions [2]. The study of the nonlinear bistability in Josephson junctions was the central topic of research in these works, a study that was continued later on via perturbation analysis with partially satisfactory results [3] until, finally, the whole analytical apparatus for the undamped, continuous-limit case was recently unveiled [4]. Nonetheless, the investigation in the area has proved to be rather rich and interesting [5, 6, 7, 8, 9, 10].

In this paper, we develop an application of nonlinear supratransmission and infratransmission to the propagation of binary information in weakly damped, discrete, finite Josephson-junction arrays, by modulating the amplitudes of the driving signal at one end. The first section of this letter introduces the mathematical model under study and the energy expressions associated with the problem, while the next section briefly presents the finite-difference schemes employed to approximate the model. A computational study to predict the occurrence of nonlinear supratransmission under the presence of external damping is carried out in the next section. Next, we study briefly some characteristics of the kinks emitted by the boundary, and the following section describes the technique employed in order to transmit binary information in discrete Josephson junction arrays, presenting a simulation of transmission. Finally, we provide a section of concluding remarks.

2. MATHEMATICAL MODEL

Throughout this paper, we assume that γ and c are nonnegative real numbers. Likewise, we consider a system $(u_n)_{n=1}^N$ of N Josephson junctions coupled through

superconducting wires, satisfying the discrete, boundary-initial-value problem

$$\ddot{u}_n - c^2 \Delta^2 u_n + \gamma_n \dot{u}_n + \sin u_n = \mu \quad (1 \le n \le N),$$

(1) subject to :
$$
\begin{cases}
u_n(0) = 0, & 1 \le n \le N, \\
\dfrac{du_n}{dt}(0) = 0, & 1 \le n \le N, \\
u_0 - u_1 = \dfrac{\phi(t)}{c^2}, & t \in (0, +\infty), \\
u_{N+1} - u_N = 0, & t \in (0, +\infty),
\end{cases}
$$

where $\gamma_n = \gamma$ for every $n < N$, and $\gamma_N = \gamma + 1/R$. The number R is called the *output reading resistance* of the system, and it is related to the output current intensity I through Ohm's law: $I = \dot{u}_N/R$. The number c will be called the *coupling coefficient*, and γ evidently plays the role of an external damping coefficient. The constant μ will be called the *Josephson current* of the system by abusing the standard terminology, and its inception in our model corresponds to a mere mathematical generalization of the model describing discrete arrays of Josephson junctions. Indeed, if μ is equal to zero, then $\phi(t)$ and I represent the input intensity function and the output current intensity, respectively, normalized to the Josephson critical current.

Notationally, $\dot{u}$ and $\ddot{u}$ denote the first- and the second-order derivatives of u with respect to time, respectively, and $\Delta_x u_n$ represents the spatial forward-difference $u_{n+1} - u_n$, while $\Delta^2 = \Delta_x \Delta_{\bar{x}}$, where the backward-difference $\Delta_{\bar{x}} = u_n - u_{n-1}$ is employed. The function ϕ may be assumed to be continuously differentiable over $(0, +\infty)$ in general. The particular case when ϕ is a sinusoidal function will be of special interest. More concretely, we will study the case when the driving is given by the function $\phi(t) = A \sin(\Omega t)$.

It is worth noticing that our mixed-value problem may be approximated via a continuous, Neumann boundary-value problem involving a perturbed sine-Gordon model for strong coupling. Also, notice that if $\gamma = \mu = 0$, then the Hamiltonian of the nth lattice site is given by

$$H_n = \frac{1}{2}\left[\dot{u}_n^2 + c^2(u_{n+1} - u_n)^2\right] + 1 - \cos u_n.$$

(2)

After including the potential energy from the coupling between the first two sites, the total energy of the system becomes

$$E = \sum_{n=1}^{N} H_n + \frac{c^2}{2}(u_1 - u_0)^2.$$

(3)

A simple integration of this formula over a finite interval of time gives the total energy injected into the system over such interval.

The limiting case consisting of the discrete Josephson-junction array with an infinite number of junctions is of particular interest. In this situation, it is easy to verify that the rate of change of the energy of the system with respect to time is provided by the formula

$$\frac{dE}{dt} = \phi(t)\dot{u}_0 - \gamma \sum_{n=1}^{\infty}(\dot{u}_n)^2.$$

(4)

3. Numerical scheme

First finite-difference scheme. We consider the system of differential equations (1), and a regular partition $0 = t_0 < t_1 < \cdots < t_M = T$ of the time interval $[0, T]$ with time step equal to Δt. For each $k = 0, 1, \ldots, M$, let us represent the approximate solution to our problem on the nth lattice site at time t_k by u_n^k, and let us convey that $\delta_t u_n^k = u_n^{k+1} - u_n^{k-1}$, that $\delta_t^2 u_n^k = u_n^{k+1} - 2u_n^k + u_n^{k-1}$ and that $\delta_x^2 u_n^k = u_{n+1}^k - 2u_n^k + u_{n-1}^k$. In order to posses discrete energy expressions that consistently approximate their continuous counterparts, the continuous-time equations will be approximated by the discrete expressions

$$
(5) \qquad \frac{\delta_t^2 u_n^k}{(\Delta t)^2} - c^2 \delta_x^2 u_n^k + \frac{\gamma_n}{2\Delta t} \delta_t u_n^k + \frac{V(u_n^{k+1}) - V(u_n^{k-1})}{u_n^{k+1} - u_n^{k-1}} = 0,
$$

for every $n = 1, \ldots, N$. Here, $V(u) = 1 - \cos u$ at any time.

Our finite-difference scheme is consistent with our mixed-value problem, conditionally stable, and possesses energy-invariant properties. More precisely, if the energy of the system at the kth time step is computed using the expression

$$
(6) \qquad E_k = \sum_{n=1}^{N-1} H_n^k + \frac{c^2}{2}(u_1^{k+1} - u_0^{k+1})(u_1^k - u_0^k),
$$

where the individual energy of the nth lattice site is computed by

$$
(7) \qquad H_n^k = \frac{1}{2}\left(\frac{u_n^{k+1} - u_n^k}{\Delta t}\right)^2 + \frac{c^2}{2}(u_{n+1}^{k+1} - u_n^{k+1})(u_{n+1}^k - u_n^k)
$$
$$
+ \frac{V(u_n^{k+1}) + V(u_n^k)}{2},
$$

then the discrete rate of change of energy turns out to be a consistent approximation for the corresponding instantaneous rate of change, while the approximations of the individual and the total energies are consistent estimates of their continuous counterparts. Particularly, the following property of consistency in the energy domain holds for every $k = 1, \ldots, M$:

$$
(8) \qquad \frac{E_k - E_{k-1}}{\Delta t} = \phi(t_k)\frac{\delta_t u_0^k}{2\Delta t} - \gamma \sum_{n=1}^{N-1}\left(\frac{\delta_t u_n^k}{2\Delta t}\right)^2.
$$

Second finite-difference scheme. It is important to observe that the energy functional H_n defined in (2) is positive definite; however, there is no guarantee that the corresponding discrete approximation given by (8) is also positive definite. In order to save that shortcoming, we present now the finite-difference scheme

$$
(9) \qquad \frac{\delta_t^2 u_n^k}{(\Delta t)^2} - \frac{c^2}{2}\bar{\delta}\delta_x^2 u_n^k + \frac{\gamma}{2\Delta t}\delta_t u_n^k + \frac{V(u_n^{k+1}) - V(u_n^{k-1})}{u_n^{k+1} - u_n^{k-1}} = 0,
$$

where $\bar{\delta} u_n^k = u_n^{k+1} + u_n^{k-1}$. The local energy at the nth node and time t_k is approximated then using the discrete expression

$$
(10) \qquad H_n^k = \frac{1}{2}\left(\frac{u_n^{k+1} - u_n^k}{\Delta t}\right)^2 + \frac{c^2}{8}\left[\left(u_{n+1}^{k+1} - u_n^{k+1}\right)^2 + \left(u_{n-1}^{k+1} - u_n^{k+1}\right)^2 \right.
$$
$$
\left. + \left(u_{n+1}^k - u_n^k\right)^2 + \left(u_{n-1}^k - u_n^k\right)^2\right] + \frac{V(u_n^{k+1}) + V(u_n^k)}{2},
$$

which is always nonnegative. Moreover, the total energy of the system is estimated through

$$(11) \qquad E_k = \sum_{n=1}^{N-1} H_n^k + \frac{c^2}{4} \left[\frac{\left(u_1^{k+1} - u_0^{k+1}\right)^2 + \left(u_1^k - u_0^k\right)^2}{2} \right].$$

This new scheme is clearly consistent with respect to problem (1) in both the solution and the energy domains. Moreover, the identity

$$(12) \qquad \frac{E_k - E_{k-1}}{\Delta t} = c^2 \left(\frac{\bar{\delta} u_0^k - \bar{\delta} u_1^k}{2} \right) \frac{\delta_t u_0^k}{2\Delta t} - \gamma \sum_{n=1}^{N-1} \left(\frac{\delta_t u_n^k}{2\Delta t} \right)^2$$

holds for every $k = 1, \ldots, M$.

Computational remarks. In order to simulate a discrete array of Josephson junctions of infinite length, we consider a finite system (1) of relatively large length N, in which each γ_n includes both the effect of external damping described above and a simulation of an absorbing boundary slowly increasing in magnitude on the last $N - N_0$ oscillators. Specifically, we let

$$(13) \qquad \gamma_n = \kappa \left[1 + \tanh \left(\frac{2n - N_0 + N}{2\sigma} \right) \right] + \gamma + \frac{1}{R} \delta_N(n),$$

where $\delta_N(n)$ is equal to 1 if $n = N$, and zero otherwise. In practice, we will let $\kappa = 0.5$, $\sigma = 3$, $N = 60$, and $N_0 = 50$.

Also, in order to avoid the generation of shock waves in a system like (1) subject to harmonic driving $\phi(t) = A \sin(\Omega t)$, we opt for increasing slowly and linearly the driving amplitude from 0 to its actual value A, during a fixed period of time about the initial instant. After that, the driving amplitude will assume the constant value A.

Both numerical methods have been employed to produce the results in this article. Our results have shown that both methods produce results that are in excellent agreement for small values of Δt, an observation that leads to conclude that the results in the following sections are intrinsic to the problem under study and not scheme-dependent.

Computationally, the implementation of these finite-difference schemes is accomplished via Newton's method, which in turn leads to implement Crout's technique with pivoting to solve tridiagonal linear systems. The stopping criterion employed in Newton's method was reached when the relative error of subsequent approximations was less than 1×10^{-6}, and the norm employed was the infinite norm in the space $\mathbb{R}^N$.

4. Analysis of supratransmission

The process of nonlinear supratransmission consists of a sudden increase in the amplitude of wave signals transmitted into a nonlinear chain by a harmonic disturbance at the end, irradiating at a frequency in the forbidden band gap. The existence of a nonlinear supratransmission threshold of the energy administered into a finite array of Josephson junctions satisfying (1) for a harmonic function ϕ and driving frequency in the forbidden band gap region $\Omega < 1$, has been established in the continuous-limit case [4] and numerically predicted for a discrete system. Using our numerical scheme, a prediction of the occurrence of nonlinear

supratransmission can be approximated for every driving frequency in the forbidden band gap of the system of equations (1), by estimating the value of the driving amplitude at which a drastic increase in the total energy of the system is detected. In the continuous-limit case, the driving amplitude A_s at which supratransmission first starts is related to Ω through the relation

$$A_s = 2c(1 - \Omega^2). \tag{14}$$

We follow next the standard methodology employed in [11], and consider several values of the damping coefficient. The results of our numerical computations are summarized as graphs of minimal amplitude at which supratransmission starts versus driving frequency, and they are presented in Figure 1. The diagram representing the undamped scenario exhibits a good agreement with the continuous prediction for high frequencies, and damping is clearly shown to delay the appearance of the supratransmission threshold for frequencies $\Omega > 0.35$.

On the other hand, the process of nonlinear infratransmission or lower transmission, as opposed to supratransmission, consists in a sudden decrease in the amplitude of wave signals in a chain harmonically driven at its end. The existence of a nonlinear infratransmission threshold under which there is a drastic decrease in the energy injected into the system was established in [4] in the continuous-limit case. As a matter of fact, the infratransmission threshold A_i is less than the supratransmission threshold A_s, and between the amplitudes A_i and A_s lies a region of bistability. In order to approximate numerically the value of A_i for a given driving frequency in the forbidden band gap with associated supratransmission threshold A_s, we chose a driving function $\phi(t) = A(t)\sin(\Omega t)$, with amplitude function defined via

$$A(t) = A_s(1 - e^{-t/\tau_1}) + (A_0 - A_s)(1 - e^{-t/\tau_2}), \tag{15}$$

where $\tau_2 \gg \tau_1$.

A finite time period of relatively large length is chosen, and a finite, undamped system consisting of 60 Josephson junctions with no Josephson current, a coupling coefficient of 5, and a driving frequency of 0.9 is fixed, for which the nonlinear supratransmission threshold is predicted to be equal 1.945, according to Equation (14). Several driving amplitudes A_0 are employed, and the total energy of the system is computed for each amplitude. The results of driving the system with an amplitude function given by (15) with $\tau_1 = 10$ and $\tau_2 = 100$ are shown in Figure 2, in which a drastic change in the behavior of the total energy with respect to A_0 is detected around the value 1.41. This value is identified as the nonlinear infratransmission threshold of the system for $\Omega = 0.9$.

As in the case of nonlinear supratransmission, the critical amplitude value at which infratransmission occurs also delays with the value of γ. More precisely, the larger the value of the damping coefficient the larger the critical infratransmission value.

5. Signal propagation

5.1. **Character of solutions.** Consider a system of 60 coupled oscillators described by (1) with coupling coefficient equal to 5, driven at a frequency of 0.9 in the forbidden band gap, and an amplitude of 2, just above the approximate supratransmission threshold. Figure 3 shows the time evolution of a kink moving away
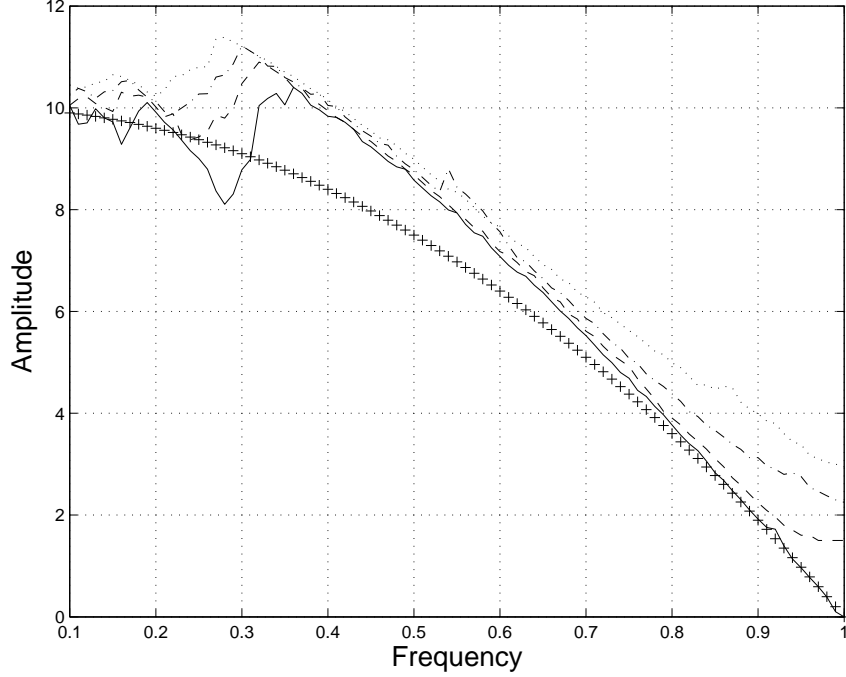
FIGURE 1. Bifurcation diagram of occurrence of critical ampli-
tude versus driving frequency for problem (1) with $c = 5$, for
$\gamma = 0$ (solid), 0.1 (dashed), 0.2 (dash-dotted), 0.3 (dotted). The
continuous-limit prediction (14) of the critical threshold is repre-
sented by a sequence of plus signs.

from the driving boundary. The exact location of the kink can be better deter-
mined by studying the time evolution of the local energies of the 60 sites at the
corresponding times.

With that purpose in mind, Figure 4 presents the evolution of the local energies
of the six snapshots in the previous figures. The location of the kinks is accurately
identified, at each individual time, as the absolute maximum of the local energies.
Moreover, a constant phase velocity of approximately 1.44 sites per unit of time is
observed.

Finally, in Figure 5 we present a simulation of the evolution of the local energies
at the same instants of time as in Figure 4. The same parametric values have been
used in both figures, except that in this last graph we employed a coefficient of
damping equal to 0.001. In this situation, our numerical results (not presented
here for the sake of briefness) show that the supratransmission threshold for this
value of γ is still smaller than the driving amplitude 2. Indeed, our results show that
there is propagation of energy in the form of localized modes; however, dissipation
of energy is present too, as evidenced by the fact that the local energy density of
localized solutions is slightly smaller when γ is not zero.

In both of the cases presented here, the group velocity of the kink produced by
the driving boundary is approximately the same: 1.44. However, the signal of the
dissipative case seems to be a little delayed with respect to the case then damping is
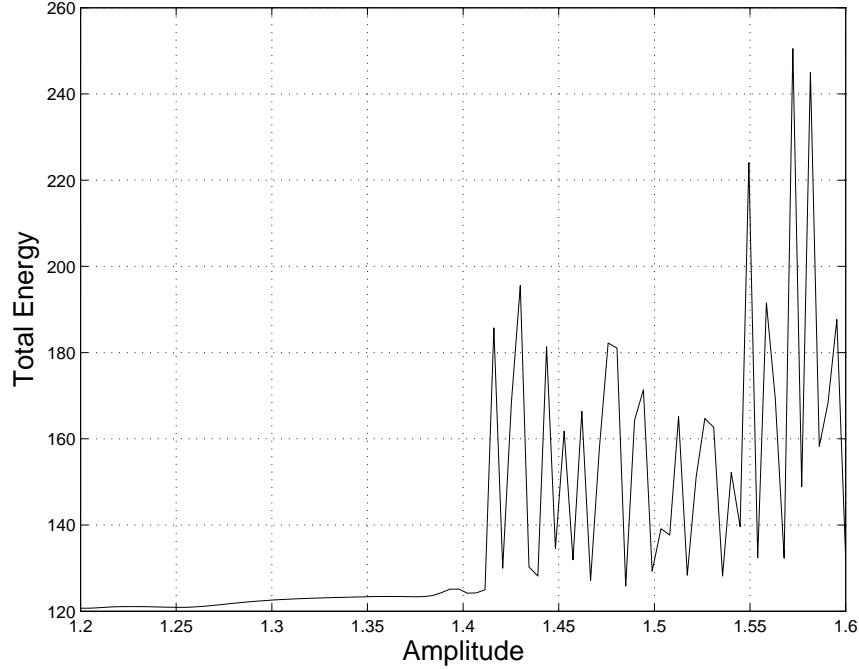
FIGURE 2. Graph of total energy vs. driving amplitude in an undamped, semi-infinite, discrete Josephson-junction array, driven at a frequency of $\Omega = 0.9$ via expression (15) during a period of time equal to 6000, with a coupling coefficient of 5.

not present. This observation is in perfect agreement with the fact that the driving amplitude A is slowly and linearly increased from 0 to 2, in order to avoid the creation of shock waves, so that the critical amplitude for the case $\gamma = 0$ is reached before the critical value for a nonzero γ.

5.2. **Simulation.** Let Ω be a frequency in the forbidden band gap of our problem. Assume that B_i and B_s are nonnegative values that are just a bit smaller than the infratransmission and supratransmission thresholds, respectively, both associated to the frequency Ω. We define the *seed* of the system as the function

$$(16) \qquad I_s(t) = \frac{1}{2}\left[(B_s - B_i)\sin(\Omega t) + B_i + B_s\right],$$

for every $t > 0$.

Next, we define the *period of signal generation* P as an integer multiple of the driving period. In our case, P will be equal to 20 times the period of driving.

Let α be a positive number with the property that $I_s(t) + \alpha$ overcomes the nonlinear supratransmission threshold for some values of t. With these conventions in mind, a single binary message $(b_1, b_2, \ldots, b_l)$ consisting of l binary bits will be transmitted into system (1). In general, for every $m = 1, 2, \ldots, l$, we define the signal function S_m by

$$(17) \qquad S_m(t) = \begin{cases} \alpha b_m \sin(\Omega t), & \text{if } mP < t < (m+1)P, \\ 0, & \text{otherwise.} \end{cases}$$
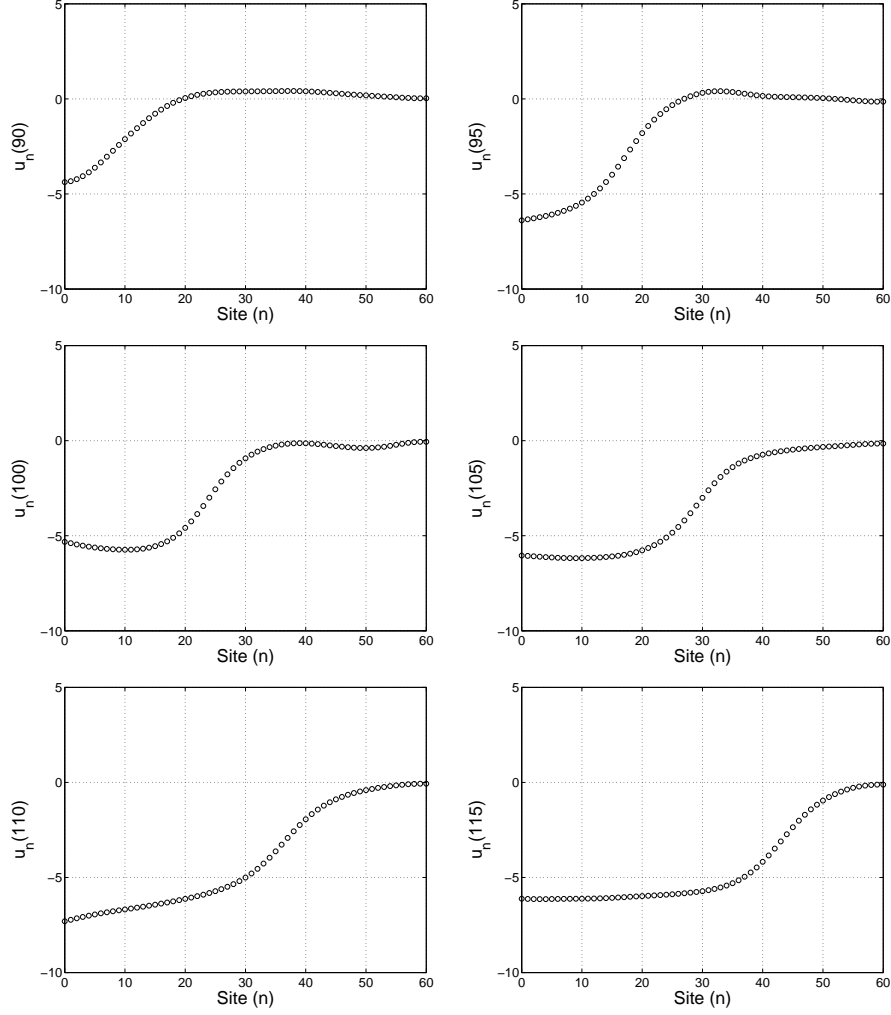
FIGURE 3. Development of a kink solution of (1) for discrete array of 60 Josephson junctions, with $\gamma = \mu = 0$ and $c = 5$, driven at the end with by a frequency $\Omega = 0.9$ and an amplitude $A = 2$ slightly above the supratransmission threshold. The snapshots were taken at 6 times equally spaced between 90 and 115, employing a step size of 0.2 and an absorbing boundary in the last 10 junctions.

The input intensity function will be defined then by

$$(18) \qquad \phi(t) = I_s(t) + \sum_{m=1}^{l} S_m(t).$$

Consider a discrete Josephson junction arrays consisting of 8 junctions with coupling coefficient equal to 2. A driving frequency $\Omega = 0.9$ will be employed, for which the values $B_i = 0.23$, $B_s = 0.41$, $\alpha = 0.05$, $\gamma = 0.002$ and $R = 10$ will be used. The binary sequence '10111001011011101001' is to be transmitted into
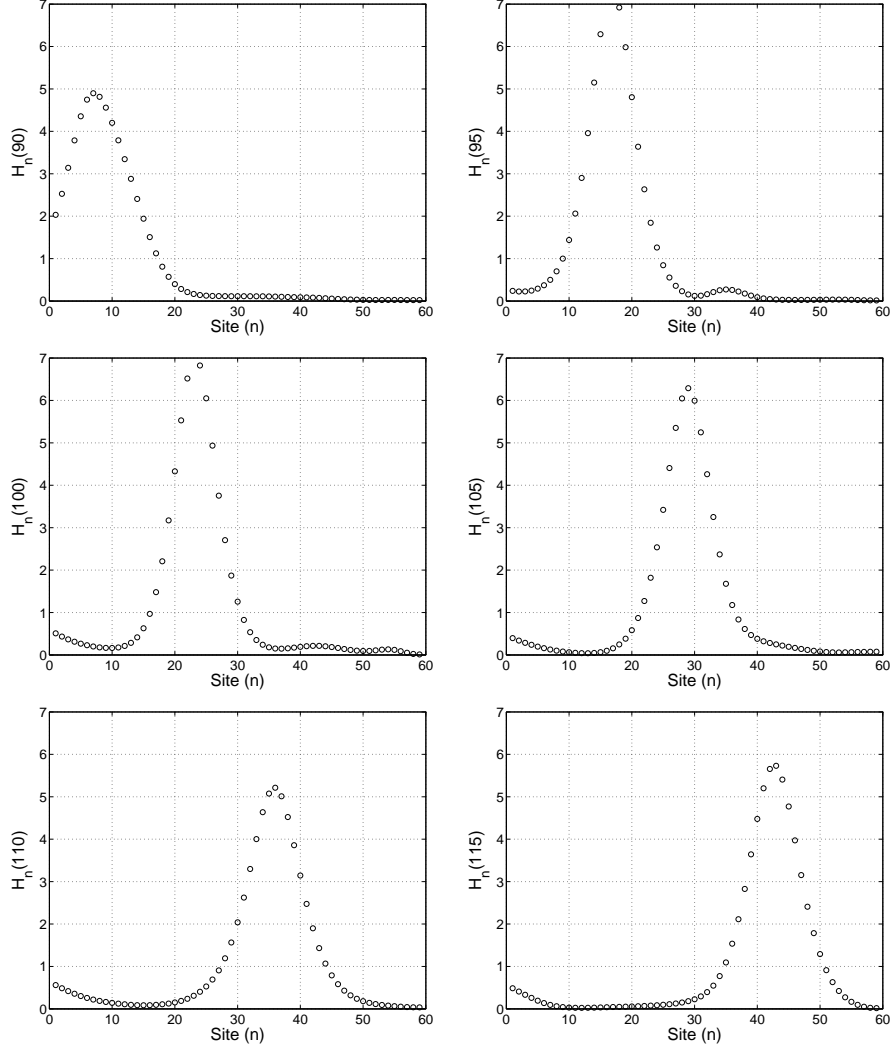
FIGURE 4. Development of the local energies in a kink solution of
(1) for discrete array of 60 Josephson junctions, with $\gamma = \mu = 0$
and $c = 5$, driven at the end with by a frequency $\Omega = 0.9$ and an
amplitude $A = 2$ slightly above the supratransmission threshold.
The snapshots were taken at 6 times equally spaced between 90
and 115, employing a step size of 0.2 and an absorbing boundary
in the last 10 junctions.

system (1) by modulating the input current intensity and read by the corresponding
output current. The resulting outcome of our simulations is summarized in Figure
6 for a normalized time.

Nonzero bits are clearly identified with output intensities of absolute values
higher than the corresponding intensities associated with bits equal to zero. More
accurately, nonzero bits are completely characterized by the fact that, at some time
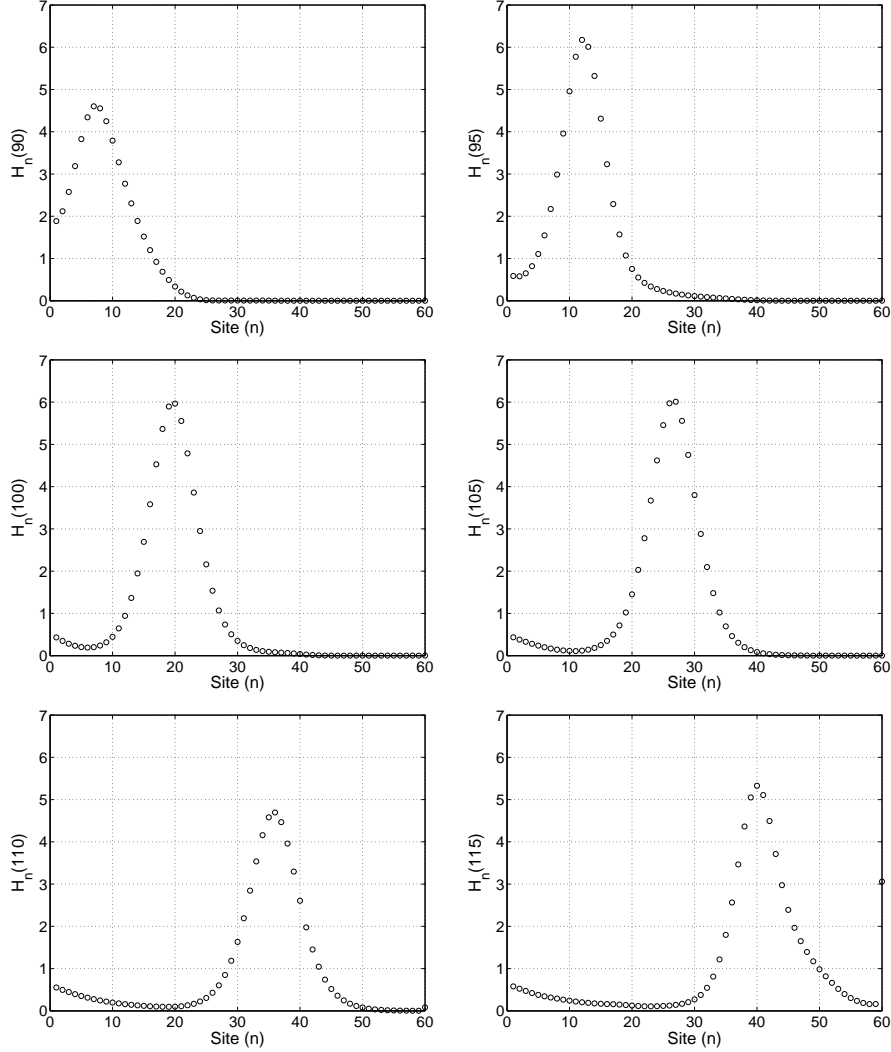
FIGURE 5. Development of the local energies in a kink solution of
(1) for discrete array of 60 Josephson junctions, with $\gamma = 0.001$,
$\mu = 0$ and $c = 5$, driven at the end with by a frequency $\Omega = 0.9$ and an amplitude $A = 2$ slightly above the supratransmission
threshold. The snapshots were taken at 6 times equally spaced
between 90 and 115, employing a step size of 0.2 and an absorbing
boundary in the last 10 junctions.

in the corresponding period of reception, the value of the intensity of the output
signal is higher than a cutoff limit (in this case equal to 0.01).

Several other experiments have been carried out for different values of γ. Here,
it is interesting to notice that our experiments have produced results which are
qualitatively in agreement with that presented in Figure 6. Particularly, it is im-
portant to mention that there is a well-defined difference between the bits 0 and 1.
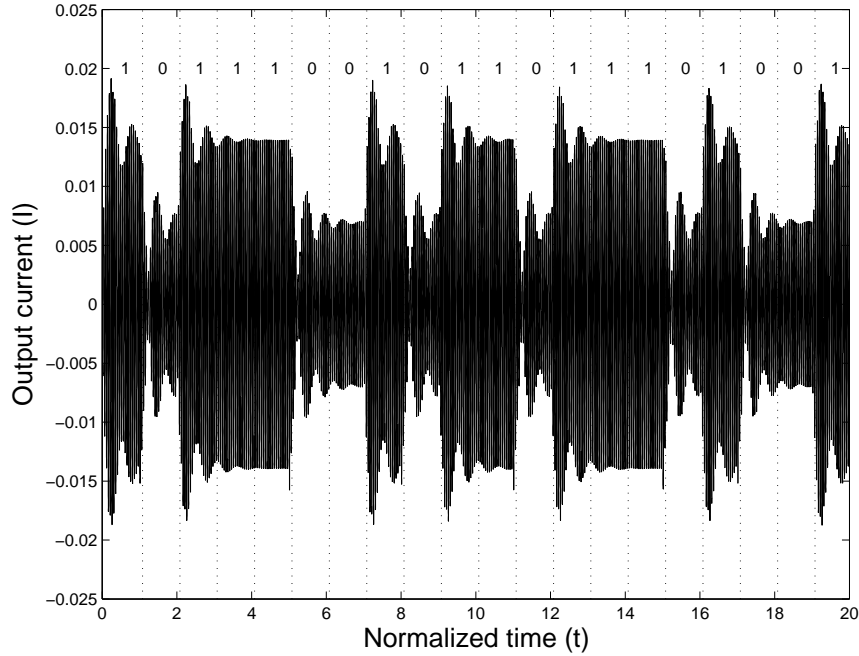
FIGURE 6. Graph of output current intensity vs. normalized time of system (1) consisting of 8 coupled junctions with $c = 2$, as a response of the input current function (18) for the binary message '10111001011011101001'. The parameters $\gamma = 0.002$, $\Omega = 0.9$ and $R = 10$ are employed.

The only difference is the amplitude of the oscillations of the output current, which decreases as γ is increased, as expected.

6. CONCLUSIONS AND DISCUSSION

In this letter, we have proved, using numerical computations, that it is possible to transmit binary information in discrete Josephson junction arrays using the processes of nonlinear supratransmission and infratransmission. In the absence of dissipative effects, our model (which is based on the modulation of amplitudes of source signals with constant frequency) has shown to be highly reliable for sufficiently long periods of single-bit generation. Moreover, our computations show that the general picture does not change much when weak damping is present; indeed, the only difference obtained between the conservative and the dissipative cases lies in the amplitude of the oscillations of the output current intensity. In practice, the knowledge of the speed at which localized solutions move through a discrete array consisting of Josephson junctions in parallel and the relation between driving amplitude, supratransmission and infratransmission thresholds and damping, may be fruitful in the accurate design of binary signal transmitters, as well as in digital amplifiers and signal detectors.

It is worth noticing the similarities and differences of our results with respect to the corresponding Dirichlet boundary-value problem. The results derived in this

paper in the supratransmission analysis for the external damping are qualitatively similar to those presented in [11]. On the other hand, the fundamental structures for transmission of wave signals in the Dirichlet scenario involved the propagation of moving breathers [12, 13]; meanwhile, kinks and anti-kinks have been generated in the Neumann boundary-value problem.

References

[1] O. H. Olsen, M. R. Samuelsen. Phys. Rev. B, 34:3510–3512, 1986.
[2] D. Barday, M. Remoissenet. Phys. Rev. B, 41:10387–10397, 1990.
[3] Y. S. Kivshar, O. H. Olsen, M. R. Samuelsen. Phys. Lett. A, 168:391–399, 1992.
[4] D. Chevrieux, R. Khomeriki, J. Leon. Phys. Rev. B, 73:214516, 2006.
[5] O. H. Olsen. Phys. Rev. E, 50:182–187, 1994.
[6] Y. S. Kivshar, O. A. Chubykalo. Phys. Rev. B, 43:5419–5424, 1991.
[7] Y. Makhlin, G. Schön, A. Shnirman. Chem. Phys., 296:315–324, 2004.
[8] Y. Makhlin, G. Schön, A. Shnirman. Physica C, 368:276–283, 2002.
[9] Y. Makhlin, G. Schön, A. Shnirman. Nature, 398:305–307, 1999.
[10] F. Geniet, J. Leon. Phys. Rev. Lett., 89:134102, 2002.
[11] J. E. Macías-Díaz, A. Puri. J. Comp. Appl. Math., 214:393–405, 2007.
[12] J. E. Macías-Díaz, A. Puri. Phys. Lett. A, 366:447–450, 2007.
[13] J. E. Macías-Díaz, A. Puri. Physics D, 228:112–121, 2007.

Departamento de Matemáticas y Física, Universidad Autónoma de Aguascalientes, Aguascalientes, Ags. 20131, Mexico
   E-mail address: `jemacias@correo.uaa.mx`

Department of Physics, University of New Orleans, New Orleans, LA 70148
   E-mail address: `apuri@uno.edu`